

UC Berkeley

UC Berkeley Previously Published Works

Title

Assessment of battery utilization and energy consumption in the large-scale development of urban electric vehicles

Permalink

<https://escholarship.org/uc/item/99t5t8q4>

Journal

Proceedings of the National Academy of Sciences of the United States of America, 118(17)

ISSN

0027-8424

Authors

Zhao, Yang
Wang, Zhenpo
Shen, Zuo-Jun Max
et al.

Publication Date

2021-04-27

DOI

10.1073/pnas.2017318118

Peer reviewed



Assessment of battery utilization and energy consumption in the large-scale development of urban electric vehicles

Yang Zhao^{a,b}, Zhenpo Wang^{a,1}, Zuo-Jun Max Shen^{b,c,d,1}, and Fengchun Sun^a

^aNational Engineering Laboratory for Electric Vehicles, Beijing Institute of Technology, Beijing, 100081, China; ^bCollege of Engineering, University of California, Berkeley, CA 94720; ^cFaculty of Engineering, The University of Hong Kong, Hong Kong SAR, China; and ^dFaculty of Business and Economics, The University of Hong Kong, Hong Kong SAR, China

Edited by John H. Seinfeld, California Institute of Technology, Pasadena, CA, and approved February 22, 2021 (received for review August 14, 2020)

Electrifying transportation in the form of the large-scale development of electric vehicles (EVs) plays a pivotal role in reducing urban atmospheric pollution and alleviating fossil fuel dependence. However, the rising scale of EV deployment is exposing problems that were previously hidden in small-scale EV applications, and the lack of large-scale EV operating data deters relevant explorations. Here, we report several issues related to the battery utilization and energy consumption of urban-scale EVs by connecting three unique datasets of real-world operating states of over 3 million Chinese EVs, operational data, and vehicle feature data. Meanwhile, by incorporating climatic data and EV data outside China, we extend our models to several metropolitan areas worldwide. We find that blindly increasing the battery energy of urban EVs could be detrimental to sustainable development. The impact of changes in the energy consumption of EVs would be exacerbated in large-scale EV utilization, especially during seasonal shifts. For instance, even with a constant monthly driving demand, the average energy consumption of Beijing light-duty EVs would change by up to 21% during winter–spring shifts. Our results may also prove useful for research on battery resources, urban power supply, environmental impacts, and policymaking.

transport electrification | battery resource | energy consumption | electric vehicle | sustainability

Large-scale electrification of transport is considered an effective solution to decrease the use of petroleum-derived fuels and mitigate the urban accumulation of air pollutants. The global stock of light-duty electric vehicles (LDEVs) exceeded 7.2 million in 2019 (1, 2), and China accounted for the largest share at ~47%, followed by Europe and the United States. To further boost the electric vehicle (EV) market, numerous jurisdictions have introduced incentives or adopted action plans: China has prolonged subsidies for EVs to 2022 (3); the European Union has provided new tax schemes for electric cars (4); and several regions in the United States and Canada, such as California and Quebec, respectively, have enacted incentives for zero-emission vehicle programs (5, 6). The International Energy Agency indicated that the global EV stock would need to increase to 140 million by 2030 (2) to achieve the goals of existing government policies [the Stated Policies Scenario (7)]. In this context, from 2019 to 2030, the global battery capacity production and electricity demand from EVs would soar ninefold to $1.5 \text{ TWh} \cdot \text{y}^{-1}$ and sixfold to $550 \text{ TWh} \cdot \text{y}^{-1}$, respectively (2, 8). Accordingly, the global demand for the critical metals used in EV batteries, including cobalt, lithium, manganese, and nickel, would increase by 8 to 14 times from 2019 to 2030 (2, 9).

The surging demand for battery resources and energy from EVs signifies a need to reassess the real-world battery utilization and energy consumption of urban-scale EVs. Research topics on this front have focused on analyzing the supply risks of battery resources (10–12), battery recycling (13–15), sustainability (16–18), charging planning (19–21), and the impact on urban power grids

(22–24). A common and indispensable input of these studies is accurate battery utilization or energy consumption of urban EVs. Meanwhile, since the environmental gains of EVs can only be measured from electricity production processes, the energy consumption of urban EVs is also an important basis for research on emissions (25–28), air pollution (29, 30), and health benefits (31, 32). However, owing to the absence of urban-scale EV operating data, most existing assessments are conducted by relying on macroscopic evaluations or the simulations that are calibrated with aggregate-level parameters (33–35). When applied to large-scale EV applications, these simplifications can lead to nonnegligible biases in the results (36) as they cannot reflect the complexity of driving trajectories and varying battery performance in EV operation. On the other hand, in small-scale EV samples, the overall levels of battery utilization and energy consumption tend to be altered by the special use behavior of individual users. This phenomenon conceals some trends that would otherwise have been evident, such as low battery utilization and seasonal changes in the energy consumption of EVs.

In 2016, the National Monitoring and Management Center for New Energy Vehicles was established in China, which serves as the national big data platform for EVs. The center has the only datasets in the world that contain real-time operating data of nationwide EVs (the number of EVs in the datasets exceeded 3 million in 2020). For the EVs in some metropolitan areas in

Significance

The surging demand for battery resources and energy from EVs signifies a need to reassess the real-world battery utilization and energy consumption of urban EVs. In this work, we incorporate unique and previously unavailable datasets of urban-scale EV operation to better understand the battery utilization and energy consumption of large-scale EV utilization. High-resolution operating data of EVs across multiple regions are collected and integrated with vehicle feature data as the input for modeling. Accordingly, we expose several issues that have nonnegligible impacts on battery resources and the urban power supply, such as low battery utilization and seasonal changes in the energy consumption of EVs. The provided models and data can be extensively utilized for further EV-related resource and energy investigations.

Author contributions: Y.Z., Z.W., Z.-J.M.S., and F.S. designed research; Y.Z. and Z.-J.M.S. performed research; Y.Z. analyzed data; Z.W. and F.S. contributed resources and analytic tools; and Y.Z. and Z.-J.M.S. wrote the paper.

The authors declare no competing interest.

This article is a PNAS Direct Submission.

Published under the PNAS license.

¹To whom correspondence may be addressed. Email: wangzhenpo@bit.edu.cn or maxshen@berkeley.edu.

This article contains supporting information online at <https://www.pnas.org/lookup/suppl/doi:10.1073/pnas.2017318118/-DCSupplemental>.

Published April 19, 2021.

China, such as Beijing and Shanghai, the coverage of the platform can reach up to 80%. The data content primarily includes two parts: dynamic vehicular data (general vehicle status, subsystem operating data, and location data) and static information (metadata and attributes). The temporal and spatial resolutions of the dynamic vehicular data are 1 to 30 s and 1 to 10 m, respectively. This large-scale and high-precision data source of Chinese EVs, coupled with EV datasets outside China, provides unique data support for achieving the large-scale assessments in this work (see *Materials and Methods*).

Here, we present a fact-based assessment of battery utilization and energy consumption in urban-scale EV applications to expose several issues affecting battery resources and the urban power supply. To this end, we combine four types of data: 1) EV operating data, 2) EV operational data describing the fleet types and license plate regions, 3) vehicle feature data providing the specifications of EVs, and 4) climate data providing ambient temperatures in different urban areas (see *Materials and Methods*). To understand the impact of regional variability, nine metropolitan areas worldwide with large EV markets (37) are selected in this work. Accordingly, we first analyze the changes in battery utilization that are affected by user behavior or limited by current battery technology. We investigate how different fleet types and climatic conditions can affect the battery utilization of urban EVs. We also display the developing trends of battery utilization in urban-scale EV groups under different directions of battery technology improvement. Then, we assess the energy consumption of urban EVs from different perspectives. We observe that in some continental climate regions, the energy consumption of EVs fluctuates greatly in different months because of temperature shifts. These fluctuations and step changes are unfavorable as they can greatly amplify the original daily energy demand of EVs, especially in urban-scale EVs. We show the extent to which this problem can be addressed as EV technology improves. The results demonstrate how often-ignored changes in the battery utilization and energy consumption of urban EVs could affect the resource efficiency of EV batteries and urban power supply.

Results and Discussion

Battery Utilization. In this section, we quantify changes in the battery utilization rates—the percentage of battery energy usage—of urban EVs. The analysis framework is shown in Fig. 1. By associating EV battery states with operational data, we observe two cases of battery utilization changes in large-scale EV groups. The first is caused by the imbalance between users' travel demand and the available driving ranges provided by EV batteries and is referred to as the behavior-related battery utilization change (38, 39). The other case is induced by the degradation in battery performance that lowers the upper limits of battery utilization rates (40–42). This case is defined as the technology-related battery utilization change as the degradation stems from the insufficiency of current battery technology. Both behavior- and technology-related changes in battery utilization can result in a waste of battery materials and an increase in costs.

Behavior-related battery utilization changes. To understand the dynamic pattern of behavior-related battery utilization in urban-scale EV groups, we first model the driving distance distributions of LDEVs at varied time scales, fleet types, and operating regions using high-resolution driving data (see *Materials and Methods*). Then, we estimate the battery utilization rates of different fleet types as a function of travel demand of the different proportions of urban LDEVs (see *Materials and Methods*). The fleet types studied in this work include two categories: public LDEVs (electric taxis and rental LDEVs) and private LDEVs. Owing to the better operational data support for EVs in China, three metropolitan areas in China with large EV markets (43) are selected in this part.

In Fig. 24, public and private fleet types show different daily driving distance distributions, whereas the three metropolitan

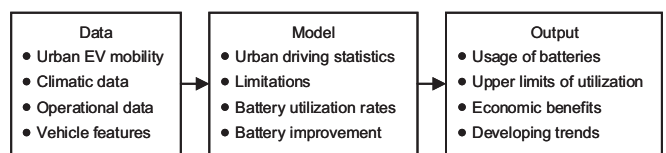


Fig. 1. Assessment framework for battery utilization. First, urban driving statistics and battery operation limitations are calculated by using urban-scale EV mobility, climatic data, operational information, and vehicle features. Second, the battery utilization model uses urban driving statistics and limitations to determine the average and upper limits of battery utilization of EVs in different regions. Third, simulations of battery improvement are incorporated into the analysis to estimate the development trends.

areas are relatively similar. In these three regions, the daily driving distance distributions of private and public LDEVs are concentrated in the ranges of 10 to 100 km and 110 to 280 km, respectively. Currently, the range of the most easily available LDEVs on the market is ~300 km (44). To meet the daily travel demand of 80% of the LDEVs in Beijing, Shanghai, and Guangzhou, the battery utilization rates of 300 km LDEVs range from 27 to 59% when used as private LDEVs and from 80 to 98% when used as public LDEVs (*SI Appendix, Fig. S1*). The data in refs. 45 and 46 also suggest that the driving distance distributions are similar in some regions in the United States and European nations, including Germany, Sweden, Seattle, and Atlanta.

In the last 2 y, EV manufacturers have tended to launch EVs with ranges exceeding 600 km (47). However, the battery utilization rates of 600 km private LDEVs are lower than 29% when needed to meet 80% of the daily travel demand in Beijing, Shanghai, and Guangzhou (*SI Appendix, Fig. S1*). These low battery utilization rates in urban-scale EVs would keep most battery materials in standby states (higher than 71%). This scale of underutilization is extremely negative for the resource efficiency of EV batteries and economic costs. Nevertheless, the decrease in behavior-related battery utilization can be avoided in some cases. For EVs with specific applications, such as taxis and buses, the main parts of their daily driving distances are normally distributed (see the distributions of public vehicles in Fig. 24). In this case, battery energy can be customized to match the daily travel demand, and this approach is positive for battery resources and costs. By contrast, the daily driving distances of urban private EVs exhibit positively skewed distributions. Hence, there is a certain percentage of users with large daily driving distances. The dispersive behavior of private EVs makes the space for optimization relatively small (48).

Technology-related battery utilization changes. We look at the decreased upper limits of battery utilization rates caused by insufficient battery technology. Nine metropolitan areas worldwide are targeted in this part. We first use statistical models to analyze the upper limits of battery utilization rates of EVs in different spatiotemporal conditions (see *Materials and Methods*). Next, we estimate the average and lowest upper limits of the battery utilization rates of EVs in varied metropolitan areas (see Fig. 2B for LDEVs and *SI Appendix, Fig. S2* for electric buses). The analysis that is carried out on data collected on a monthly basis is utilized to assess the impact of seasonal shifts (Fig. 2C and *SI Appendix, Fig. S3 A–F*). Interestingly, we find that several regions with oceanic climate characteristics, such as Los Angeles and London, may have relatively high upper limits of battery utilization rates (greater than 84%; see the lowest battery utilization rates in Fig. 2B and ambient temperatures in *SI Appendix, Fig. S4 A–J*). By contrast, in several continental climate regions, such as Beijing and New York, their low winter temperatures lower the upper limits of battery utilization rates by up to 35 to 43%.

We then use highly resolved EV data to investigate how seasonal changes could affect users' actual behavior with respect to

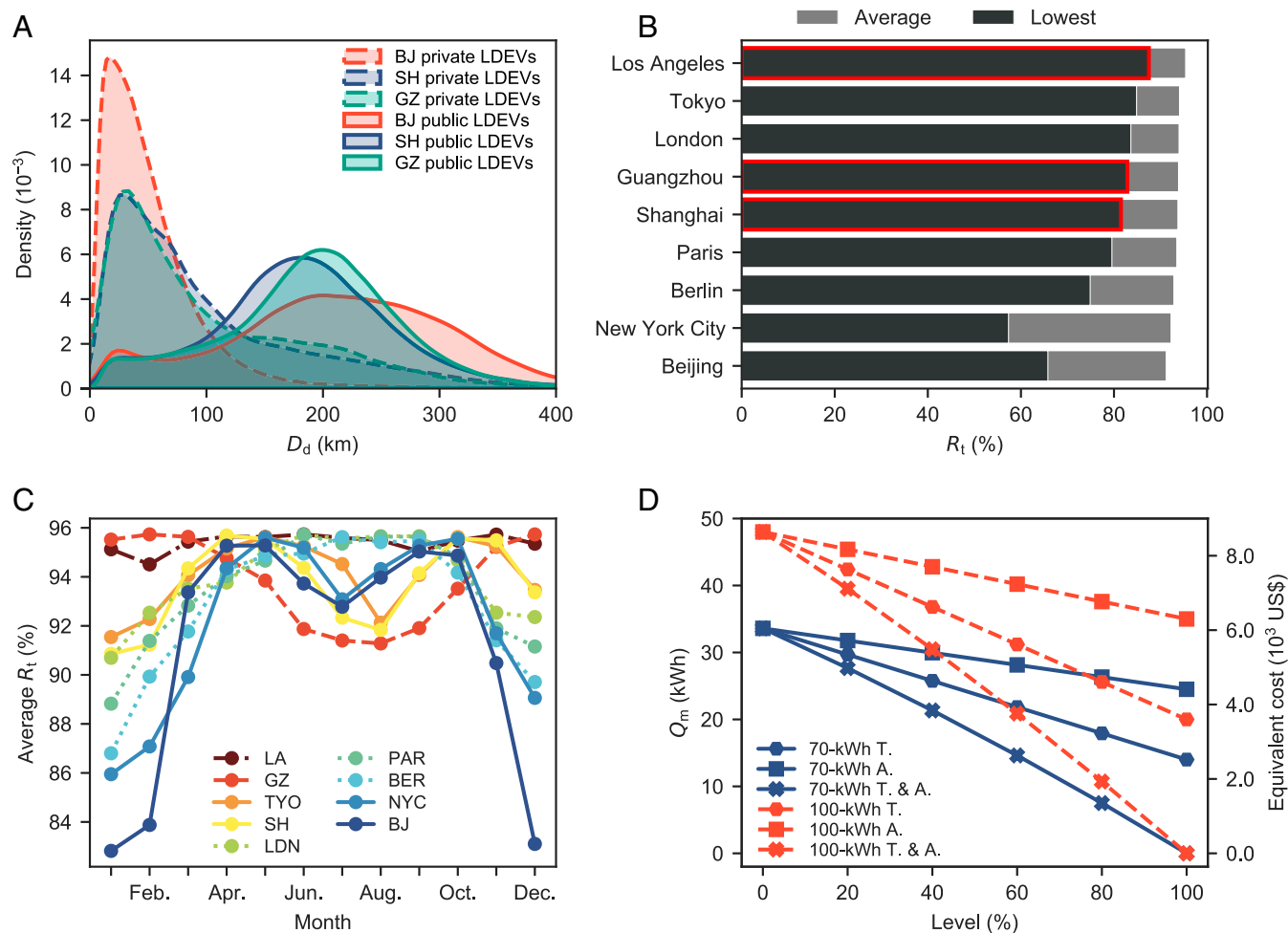


Fig. 2. Assessing battery utilization. (A) Daily driving distance distributions in six categories (three metropolitan areas: Beijing, Shanghai, and Guangzhou; and two fleet types: public and private LDEVs). (B) Annual average and lowest upper limits of battery utilization rates, R_t , of LDEVs in nine regions. The bars marked in red indicate that the lowest value occurs in summer. (C) Monthly average upper limits of battery utilization rates of LDEVs in nine regions. Four line styles represent four patterns of the changes in average R_t : only decrease in summer (GZ) or winter (LON, PAR, and BER), decrease in both summer and winter (TYO, SH, NYC, and BJ), and almost no decrease (LA). (D) Maximum unavailable battery energy, Q_m , and equivalent battery costs of LDEVs in Beijing with varied battery energy (70 kWh and 100 kWh) under individual or combined (T. & A.) battery improvement of improving extreme temperature performance (T.) and reducing aging effects (A.).

EV batteries. In *SI Appendix, Fig. S5*, it can be seen that the average state of charge (SOC) of LDEVs starts to decrease in the 6:00 to 8:00 morning period and reaches a minimum at ~22:00 to 23:30 (subsequent charging would increase the SOC). Interestingly, we find that in some regions, more battery capacity is needed to meet the driving demand of EVs in winter. From the SOC distributions in *SI Appendix, Fig. S5 A–L*, it can be observed that for the targeted Beijing LDEV group, low SOC values occur more frequently during the winter months. *SI Appendix, Fig. S6* shows that for the Beijing LDEV group, the daily average SOC ranges from 69 to 71% in winter and from 71 to 76% in other seasons, while the daily average SOC of Guangzhou LDEVs ranges from 67 to 70%, reaching the lowest value in summer. These trends and the months when the extreme values occur are similar to the changes in the upper limits of battery utilization rates (Fig. 2C and *SI Appendix, Fig. S6*). Based on these, we may infer that seasonal changes have already been affecting the battery usage and charging behavior of large-scale EV applications (changes in energy demand are discussed in a later section).

We evaluate the impact of decreased upper limits of battery utilization rates on the waste of battery materials and increased economic costs, considering different levels of battery improvement. To this end, we calculate the largest portion of unavailable

battery energy that is caused by the degradation in battery performance, namely, the maximum unavailable battery energy. We perform linear simulations of three aspects of battery improvement that can reduce the impact on battery performance degradation: reducing aging effects (49), improving performance at high and low temperatures (50, 51), and increasing battery energy densities (52). For the first two aspects, we define a development level of 0% to represent the current level and a level of 100% to indicate that this aspect will have no restrictions on battery utilization (see *Materials and Methods*). Regarding the battery energy density, we simulate the varied battery energy densities of current EVs. As shown in Fig. 2D, the maximum unavailable battery energy of Beijing LDEVs with 70 kWh batteries can reach 33.6 kWh. In this case, if the restrictions induced by extreme ambient temperatures or battery aging are reduced by 80%, the unavailable battery energy can be curtailed by up to 15.7 kWh or 7.3 kWh, respectively. The equivalent economic benefits realized by optimizing battery packs reach \$2,826 or \$1,314, respectively (see cost calculation in *Materials and Methods*). Further results for LDEVs in more regions are displayed in *SI Appendix, Fig. S7 A–I*. It can be seen that although the impact of climatic conditions varies in different regions, LDEVs with

higher battery energy will always suffer higher maximum unavailable battery energy.

Moreover, since the battery materials needed to manufacture an electric bus are substantially more than an LDEV, ensuring high battery utilization rates of electric buses is more significant for battery material sustainability. To save the costs of procuring electric buses, bus operators tend to order electric buses whose battery sizes are reduced as much as possible under the premise of meeting a basic daily travel demand. As electric buses generally have fixed application scenarios (routes and schedules), it is significant for them to reduce the portion of battery energy that can become unavailable when batteries are under high and low ambient temperatures or aging. *SI Appendix, Fig. S8A* shows that the maximum unavailable battery energy of electric buses with 150 kWh battery packs in Beijing can reach 65.2 kWh, and the equivalent cost can reach \$9,128. We show the results for electric buses in more regions in *SI Appendix, Fig. S8 B–I*. Overall, we conclude that there are certain differences in battery utilization for different operating regions, fleet types, and battery technology levels. However, in any case, if the battery energy of EVs is unnecessarily increased, more battery materials would be underutilized (results with varied battery energy are compared in Fig. 2D and *SI Appendix, Figs. S7 and S8*).

Energy Consumption. Our goal in this section is to assess changes in the energy consumption of urban EVs by examining different operating regions, time scales, fleet types, and group scales. The assessment framework is displayed in Fig. 3. First, we investigate the energy consumption rates (ECRs)—energy consumption per kilometer—of EVs in different spatiotemporal conditions (see *Materials and Methods*). Next, we use the ratio and relative increase of the actual and average lowest ECRs to compare the average levels of the ECRs of EVs across nine metropolitan areas. Fig. 4A depicts the annual average and highest ratios of LDEV ECRs in nine metropolitan areas. The annual average ECRs of LDEVs in Beijing and New York City are 6.5 to 8.5% higher than the lowest ECRs, and the highest ECRs can increase by 68.3%. By contrast, the temperature conditions of Los Angeles and Guangzhou are more conducive to EV battery operation. In these two regions, the annual average and highest ECR increases for LDEVs are less than 4.6 and 24.2%, respectively. The regional differences in the relative increases of ECRs for electric buses exhibit a similar pattern to those of LDEVs (*SI Appendix, Fig. S9*). Note that the highest ECRs of LDEVs in Guangzhou occur in summer (marked in red in Fig. 4A), while those in the other eight regions occur in winter.

To understand why the highest ECRs of LDEVs occur in different seasons, Fig. 4B contrasts the monthly average energy consumption of power and auxiliary systems of LDEVs in two representative regions: Beijing (temperate continental climate) and Guangzhou (subtropical climate). For the LDEVs in Beijing, the low winter temperature (average below 0 °C) not only decreases the battery performance but also increases the energy consumption of auxiliary systems [more electricity for cabin heating

(53)]. This combined effect produces the highest ECRs of Beijing LDEVs in winter. On the other hand, the average winter temperature in Guangzhou is relatively high (average above 15 °C), which would not explicitly curtail EV battery performance (51). However, the average ECRs of Guangzhou LDEV auxiliary systems in summer are almost double those in spring [hot weather leads to higher energy consumption of air conditioners (53, 54)], which makes their overall ECRs peak in summer.

From a monthly perspective, we analyze the impact of operating regions and group scales on the monthly energy consumption of urban EVs. We first estimate the monthly average ECRs of LDEVs in nine regions (*SI Appendix, Fig. S10*) and monthly driving distance distributions in three regions (see Fig. 6A, *Inset*). Accordingly, we investigate the average impact of the scale increase of urban EVs on the urban monthly power supply. *SI Appendix, Table S1* illustrates that in Beijing, an increase of 2 million private LDEVs, 0.4 million public LDEVs, or 0.13 million electric buses (10 m in length) would increase the urban monthly power supply by ~10%. On the other hand, we observe that in some regions, even with a constant monthly driving demand, there are still significant changes in the energy consumption of urban EVs during winter–spring and autumn–winter seasonal shifts (e.g., up to 21% in Beijing and 13% in New York City; see *SI Appendix, Fig. S11 A–J*). This is primarily induced by the evident changes in ECRs caused by rapid regional temperature changes (53). For example, in Beijing, the average ECR of LDEVs fluctuates greatly throughout the year, rising by 26.7% in January and plummeting to the lowest ECR in May (Fig. 4C). By contrast, in Los Angeles, where the ambient temperature is highly even, the changes in the average ECR of LDEVs are fairly stable, varying less than 5% throughout the year (*SI Appendix, Figs. S4 A–I and S11E*). These results highlight the strong regional characteristics of EV monthly energy consumption. Moreover, we analyze how the scale increase of urban EVs affects the energy demand changes during seasonal shifts (*SI Appendix, Fig. S12 A–C*). Fig. 4D shows the maximum increase and decrease in monthly energy consumption of the public LDEVs versus the group scale in the different regions. The curves indicate that significant changes would be exacerbated as electrified transportation rapidly develops. The results in *SI Appendix, Fig. S13* suggest that these changes can be attenuated when the high and low temperature performance of EVs is improved (54).

We then explore how seasonal changes could affect the real-world charging behavior and charging loads of urban LDEVs. Fig. 5 shows the minute-level changes in the number of active EVs (charging and driving) in an EV group for different seasons (the maximum value is standardized as 1,000 EVs for comparison). It can be seen that the maximum number of LDEVs in driving and charging states, respectively, takes place in the 9:00 to 11:00 morning period and 23:00 to 1:00 midnight period. The average ratio (R_{dc}) between the number of charging LDEVs and the number of driving LDEVs is calculated to compare the intensity of charging activities for different months. As shown in *SI Appendix, Fig. S14 A–L*, for Beijing LDEVs, the values of R_{dc} in January and July are 0.25 and 0.23, respectively, evidently higher than those in other months (0.1 to 0.22); the values of R_{dc} for Guangzhou LDEVs, however, are less variable, ranging from 0.23 to 0.25. *SI Appendix, Fig. S15* presents the charging loads of LDEVs in a day for different months. It can be observed that the daily average charging load of LDEVs in Beijing peaks in January and that of LDEVs in Guangzhou peaks in July. By combining the results of active LDEV numbers and the charging loads, we find that there are more cases of recharging for Beijing EVs in the afternoon in winter, which leads to a higher power demand during this period (Fig. 5D and *SI Appendix, Figs. S14 and S15*). Note that although seasonal changes in some regions may affect the power supply of EVs, there is no evidence that it determines when power peaks occur. More imperative factors,

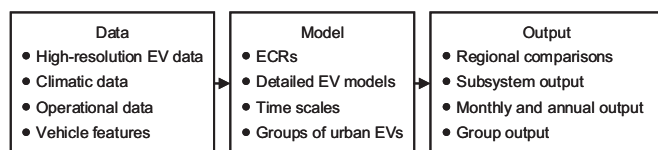


Fig. 3. Assessment framework for energy consumption. First, the energy consumption model uses real-world EV data to measure the ECRs of large-scale urban EVs in varied circumstances. Second, the detailed EV model uses these results to calculate subsystem energy consumption. Third, by modeling at different time scales and group scales, the model generates results from monthly, annual, and group perspectives.

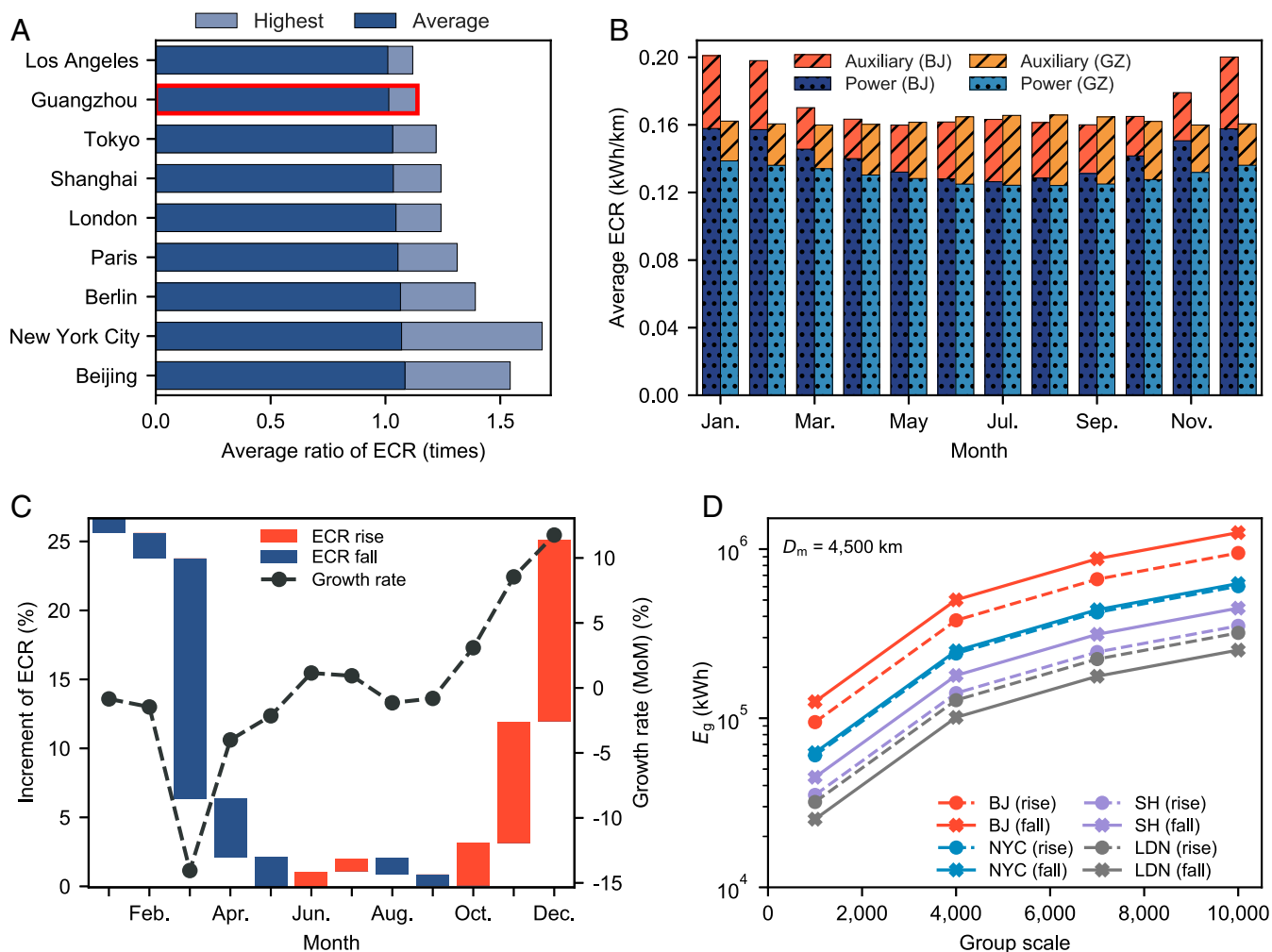


Fig. 4. Regional and monthly changes in EV energy consumption. (A) Annual average and highest ratios of ECRs in nine regions. The bar marked in red indicates that the highest value occurs in summer. (B) The average ECRs of the power and auxiliary systems of the LDEVs in Beijing and Guangzhou. (C) The increments and month-over-month (MoM) growth rates of the LDEV ECR in Beijing. The ECR increments are defined as the relative increases between monthly average ECRs and the lowest ECRs. The red and blue bars represent an ECR increase and decrease, respectively. (D) The maximum monthly energy consumption changes E_g between 2 consecutive months of the urban EV groups with increasing group scale under a fixed monthly driving distance D_m .

such as charging coordination, may have more direct impacts on the peak generation (19, 23).

For long-term EV operation, we look at the annual energy consumption of urban EVs. To better understand its changes from a holistic and development perspective, more variables are included: operating regions, group scales, fleet types, and the improvement of EV performance at high and low temperatures (53, 54). The analyses in this part are primarily conducted for EVs in Beijing, Shanghai, and Guangzhou. For the performance improvement, we define a development level of 0% to represent the current level and a level of 100% to indicate a situation where the ambient temperature has no impact on the ECRs of EVs. Accordingly, we first analyze how this performance improvement can affect the annual energy consumption of EVs. Since the annual energy consumption is linearly related to the average monthly driving distance, public LDEVs with an average monthly driving distance of $\sim 4,500$ km are used as an example (Fig. 6A, Inset). Fig. 6A displays that the average annual energy consumption of current public LDEVs in Beijing, Shanghai, and Guangzhou is $\sim 9,374.2$ kWh, 8,937.1 kWh, and 8,767.1 kWh per vehicle, respectively. In this case, if the energy consumption increases induced by high and low temperatures are reduced by 80% (corresponding to the development level of

80%), the annual energy consumption of public LDEVs in these three regions can be curtailed by 587.4 kWh, 237.7 kWh, and 101.7 kWh per vehicle, respectively. The figures for nine regions and more scenarios are compared in SI Appendix, Fig. S16 A–D. By combining these results, we also infer that EVs with higher travel demand or frequently operating at high and low temperatures may benefit more from the improvement.

We evaluate the impact of the varied fleet types and group scales on the annual energy consumption of LDEV groups. As shown in Fig. 6B, for every additional 1,000 LDEVs in Beijing, Shanghai, or Guangzhou, the marginal increases in groups' annual energy consumption peak between 8.6 and 9.8 GWh when all vehicles are intended for public use. The increases induced by the growth of private LDEVs in the three metropolitan areas are only 19.6, 50.3, and 43.7% of those of public LDEVs. Interestingly, the annual energy consumption of private LDEVs in Beijing is lower than that in Shanghai and Guangzhou, though the ambient temperature in Beijing is more unfavorable to EV operation (Fig. 6B and SI Appendix, Fig. S4 B and I). A reasonable explanation is that the average monthly driving distances of private LDEVs in Beijing are usually smaller than those in the other two regions (Fig. 6A, Inset). This explanation further suggests that, unlike the monthly energy consumption, the annual energy consumption of urban EVs

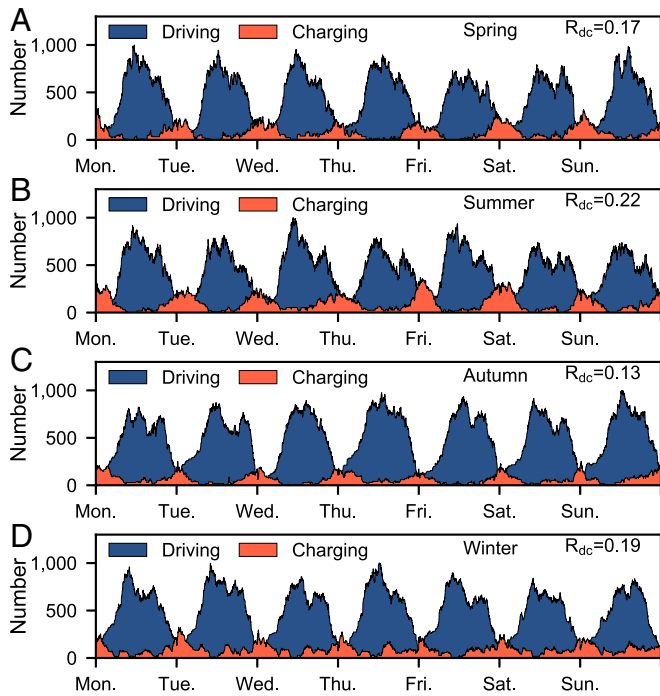


Fig. 5. Number of charging and driving vehicles in an LDEV group for different seasons in Beijing. *A*, *B*, *C*, and *D* represent the results of spring, summer, autumn, and winter, respectively. The maximum value is standardized as 1,000 EVs for comparison; the temporal resolution is 1 min. The factor (R_{dc}) represents the average ratio between the number of charging EVs and the number of driving EVs.

is determined more by their average monthly driving distances than their operating regions.

Conclusions

As the scale of transport electrification continues to increase worldwide, research has focused on battery resources and the power supply of urban EVs. Our assessment incorporates unique and previously unavailable datasets of actual urban-scale EV operation to provide a better understanding of the battery utilization and energy consumption of large-scale EV utilization. Given the illustrated variation induced by operating regions, group scales, fleet types, and time scales, existing macroscopic and aggregate-level evaluations in this field should be avoided in decision making as the simplifications can yield misleading results.

We assess two types of observed battery utilization changes in large-scale EV operation, namely, behavior- and technology-related battery utilization changes. Surprisingly, both cases display fairly low battery utilization rates in an urban scope. For instance, in Beijing, only an average of 13% of battery energy is employed daily in 600 km private LDEVs, and up to 35% of battery energy cannot be utilized temporarily or permanently because of insufficient battery technology. In this context, blindly increasing the battery energy of urban EVs will decrease the efficiency of battery resources. Moreover, the results of a regional comparison reveal that restrictions on battery utilization are greater in regions where extremely high or low ambient temperatures usually occur. Relatively delaying the large-scale development of EVs in these regions would be positive for the sustainability of battery materials and the economy.

In terms of energy consumption, the presented results exhibit the nonnegligible impact of the growing scale of urban EV utilization on the urban power supply. For example, electricity generation in Beijing would increase by 10% with an increase of ~0.4 million public LDEVs or 2 million private LDEVs. On the

other hand, even with a constant monthly driving demand, there are significant changes in the energy consumption of urban-scale EVs during seasonal shifts (for instance, up to 21% in Beijing and 13% in New York City). These changes are undesirable for the power grid and would be exacerbated when EVs become the majority of urban transportation. Furthermore, the described comparison indicates that the average monthly driving distance would be the most decisive factor for the long-term energy consumption of urban EVs.

Our work represents an important step toward the resource and energy assessment of large-scale urban EV applications. The provided methods and data can be widely utilized as the basis of high-precision modeling for future research on resources, energy management, power grids, and emissions. In addition, the presented evaluation models are built based on statistical methods and therefore applicable to nearly all types of battery-based transport.

Materials and Methods

Data. The real-world data of EVs in China utilized in this paper are obtained from the National Monitoring and Management Center for New Energy

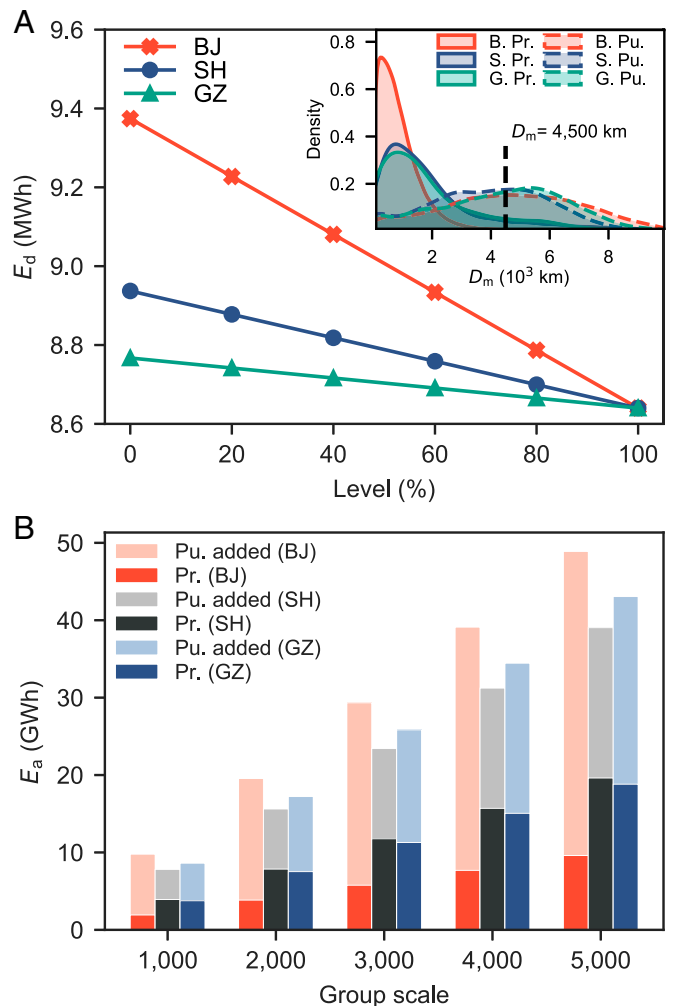


Fig. 6. Assessing annual energy consumption of EVs. (A) Annual energy consumption per public LDEV, E_d , in three regions with varying improvement levels of EV high- and low-temperature EV performance. (Inset) The distributions of the monthly driving distances of the public/private fleet types in Beijing, Shanghai, and Guangzhou. (B) Annual energy consumption of the LDEV groups, E_a , in three regions with increasing group scale. The added parts of public LDEVs represent the situation where the share of public LDEVs in the group is increased from 0 to 100%.

Vehicles and the National Big Data Alliance of New Energy Vehicles (NDA-NEV) Open Lab. The data center contains real-time EV data of more than 3 million EVs, and the data sources used for modeling primarily comprise two categories: dynamic and static datasets. The dynamic datasets primarily include EV operating data, such as the timestamp, vehicle velocity, total driving distance, and location data (latitude and longitude). For dynamic data, the temporal resolution is between 1 and 30 s, and the spatial resolution is between 1 and 10 m. The static datasets encompass EV operational data and vehicle feature data, such as fleet types, regions to which the license plates belong, etc. The classification of the types of the data is illustrated in *SI Appendix, Fig. S17*. The operating data of EVs are transmitted according to protocol GB/T 32960 and stored in the data center by using big data technologies. Subsequently, EV data are preprocessed (classified, filtered, etc.) to provide inputs for further statistical analyses. The EV data used can be freely downloaded (see *Data Availability*). The real-world EV data outside China are collected from open datasets (55, 56) and research (19, 53, 54, 57). The vehicle specification datasets are acquired from the open databases of EV manufacturers and the Ministry of Industry and Information Technology of China. The urban electricity generation data are obtained from the National Bureau of Statistics of China (58). The climate data of regions worldwide used in this paper are collected from open datasets of Weather Underground (<https://www.wunderground.com/>) and Reliable Prognosis (<https://rp5.ru/>).

Driving Distance Distributions. To incorporate real-world driving demand into the analysis, we extract the distributions of daily and monthly driving distances by using real-world records of EV operation. Since there could be more than one driving session in a day, multiple driving sessions of a vehicle are integrated to compute the daily driving distance. In this work, the daily driving distance is obtained by calculating the difference between the last and first odometer values of the day. Then, daily driving distance records are labeled with dates, regions, fleet types, and anonymous vehicle identifications to acquire daily driving distance sets in designated regions and of targeted fleet types. Monthly driving distances are calculated by aggregating daily driving distances. For both the daily and monthly driving distances, the cumulative distribution function $F^{r,t}$ for a specific region r and fleet type t is

$$F^{r,t}(x) = \sum_{u=\varepsilon}^x f_{\Delta}^{r,t}(u), \quad [1]$$

where $f_{\Delta}^{r,t}(u)$ is the share of vehicles in the driving distance interval $(u, u + \Delta]$, and ε is the threshold of the daily or monthly driving distance.

Battery Utilization Models. We define EV battery utilization rates as the percentage of battery energy utilized for driving. By employing the strong linear relationship between consumed battery energy and driving distances in statistics (*SI Appendix, Fig. S18*), we transform the calculation of battery energy usage into that of the driving range usage. In terms of the behavior-related battery utilization rate $R_b^{r,t}$ of region r and fleet type t , the equation is given as follows:

$$R_b^{r,t}(\phi) = d_u^{r,t}(\phi)/d_o, \quad [2]$$

where ϕ is the proportion of urban vehicles to be covered, $d_u^{r,t}(\phi)$ is the driving range that can cover the daily driving demand of the specified share ϕ of urban vehicles in fleet type t and region r , and d_o is the official range of the target EVs. Note that $d_u^{r,t}$ can be derived from a simple transformation of the driving distance distribution.

For technology-related battery utilization changes, we aim to measure the maximum proportion of battery energy that is available or unavailable for driving. However, in real-world operation, it is practically impossible to deplete all battery energy of EVs, and EVs are usually charged or discharged irregularly. In this context, we normalize the operating conditions by considering a trade-off between being able to cover as many use scenarios as possible and ensuring that the number of eligible records is sufficient to be statistically significant. In *SI Appendix, Fig. S19*, it can be seen that the SOC interval [35, 95] covers ~87% of total SOC usage and that further expansion of this interval has relatively small marginal gains (only an increase of 6% in coverage when changing from [35, 95] to [10, 95]). In this work, a fixed SOC interval, from 95 to 35%, is chosen for normalization. Based on this approach, the upper limit of the battery utilization rate for each trip, $R_{trip}^{r,m,v}$, is calculated as follows:

$$R_{trip}^{r,m,v} = d_{trip}^{r,m,v} / d_{int}^v, \quad [3]$$

where r , m , and v are the parameters of the region, month, and vehicle type, respectively, $d_{trip}^{r,m,v}$ is the tailored driving distance of a trip that meets the SOC

interval condition, and d_{int}^v is the equivalent official driving range in the designated SOC interval. By aggregating the battery utilization rates of individual trips in different dimensions, we calculate the average upper limits $R_c^{r,m,v}$ of the battery utilization rates of EVs in region r , month m , and vehicle type v . That is,

$$R_c^{r,m,v} = \sum R_{trip}^{r,m,v} / N, \quad [4]$$

where N is the total number of trips. In addition, a general model for urban average upper limits of battery utilization rates is provided by using the available driving range ratios and regional ambient temperatures (*SI Appendix, Figs. S20A and S21A*). The reduction of available ranges from 25 to -5 °C in this model is ~26%, which is in line with the results in refs. 53 and 59. To analyze the contribution of battery improvement to battery material efficiency, we estimate the changes in the maximum unavailable battery energy Q_m and the equivalent battery cost C_{eq} . That is,

$$\begin{bmatrix} Q_m \\ C_{eq} \end{bmatrix} = Q_o \times f_e(\theta, \mathbf{R}_i) \begin{bmatrix} 1 \\ \mu \end{bmatrix}, \quad [5]$$

where Q_o is the official battery energy, θ is the development level vector for different battery technology directions, \mathbf{R}_i is the vector of the lowest upper limits of the battery utilization rates in region r , μ is the coefficient of the equivalent cost given in *SI Appendix, Table S2*, and f_e is the function of the percentage of the maximum unavailable battery energy, as detailed in *SI Appendix*.

Energy Consumption Models. To measure the electricity consumed by EVs from the power grid per kilometer, we define the ECR (δ_{trip}) of each trip as follows:

$$\delta_{trip} = E_c / D_{trip}, \quad [6]$$

where D_{trip} is the driving distance of the trip and E_c is the charged energy in the adjacent charging process (the SOC intervals of the driving and charging processes are controlled to be the same). By linking different datasets, all computed ECR results are labeled with the corresponding operating attributes (such as the location and starting time), climatic conditions (such as the ambient temperature), operational status (such as the fleet type), and vehicle features (such as the vehicle type and battery type). Therefore, the average ECRs of EVs in varied circumstances are acquired by applying conditional aggregation on the labeled ECR datasets. In addition, a general model for the average ECR changes of urban EVs is provided in *SI Appendix, Figs. S20B and S21B*. To analyze the average energy consumption of power and auxiliary systems from a monthly perspective, we acquire the subsystem ECR matrix using the following formulation:

$$\begin{bmatrix} \delta_{aux}^{r,1} & \delta_{pow}^{r,1} \\ \vdots & \vdots \\ \delta_{aux}^{r,12} & \delta_{pow}^{r,12} \end{bmatrix} = \begin{bmatrix} \delta_{avg}^{r,1} & 0 \\ \vdots & \ddots \\ 0 & \delta_{avg}^{r,12} \end{bmatrix} \begin{bmatrix} \varsigma_{aux}(\kappa^{r,1}) & \varsigma_{pow}(\kappa^{r,1}) \\ \vdots & \vdots \\ \varsigma_{aux}(\kappa^{r,12}) & \varsigma_{pow}(\kappa^{r,12}) \end{bmatrix}, \quad [7]$$

where $\delta_{aux}^{r,m}$ and $\delta_{pow}^{r,m}$ are the ECRs of the auxiliary and power systems, respectively, in region r and month m ; $\delta_{avg}^{r,m}$ is the average ECR of the target EVs; ς_{aux} and ς_{pow} are functions of the energy consumption shares of the auxiliary and power systems, respectively, and are derived from actual subsystem data; and $\kappa^{r,m}$ is the ambient temperature. The changes in the number of active EVs are generated by counting the vehicle numbers (in driving or charging states) at different time intervals. In this case, the temporal resolution is controlled to be 1 min, and the maximum number of EVs is standardized as 1,000 for comparison. To reflect the intensity of charging activities, the average ratio (R_{dc}) between the numbers of charging and driving EVs in an EV group is calculated. The methods in ref. 60 are used in the calculation for charging load profiles. We estimate the annual energy consumption of EVs considering different operating regions, fleet types, and the improvement levels of the high/low-temperature EV performance. First, to compare the results in varied regions, the monthly driving distances of EVs are controlled to be the same. The average annual energy consumption E_d^r of EVs in region r with improvement level θ_t can be written as follows:

$$E_d^r(d_m, \theta_t) = \sum_m f_c(\theta_t, \delta_{avg}^{r,m}) \times d_m, \quad [8]$$

where d_m is the monthly driving distance and f_c is a function to convert the current ECR to the future ECR when the EV technology is improved as detailed in *SI Appendix*. We then calculate the energy consumption of the EV groups of public and private LDEVs with increasing group scale. The monthly energy consumption of an LDEV group is determined by the share of the different fleet types, ECRs, and driving distance distributions. The monthly

and annual energy consumption, $E_m^{r,m}$ and E_a^r , respectively, of an LDEV group in region r can be written as follows:

$$E_m^{r,m}(n) = n \times \int_{\alpha}^{\beta} u \times \delta_{avg}^{r,m} \times \sum_{i \in V} [p_i \times f_i^r(u)] du \quad [9]$$

and

$$E_a^r = \sum_m E_m^{r,m}, \quad [10]$$

where n is the scale of the group, α and β are the specified lower and upper limits of monthly driving distances, respectively, V is the set of all fleet types, p_i is the proportion of fleet type i in the group, and f_i^r is the probability

density function of the monthly driving distance distribution of fleet type i in region r .

Data Availability. The data and code used in this paper have been deposited in the GitHub repository (https://github.com/zhybit/Urban_EV_Assessment). All study data are included in the article and/or *SI Appendix*.

ACKNOWLEDGMENTS. We gratefully acknowledge the feedback from Professor May R. Berenbaum (Editor-in-Chief) and two anonymous reviewers, which helped improve this work. This research is partially supported by the National Key R&D Program of China (Grant 2019YFB1600800) and the National Natural Science Foundation of China (Grants 71991462 and 91746210).

1. R. Irlle, Global BEV & PHEV sales for 2019. <http://www.ev-volumes.com/country/world-world-plug-in-vehicle-volumes/>. Accessed 1 June 2020.
2. IEA, Global EV outlook 2020. <https://www.iea.org/reports/global-ev-outlook-2020>. Accessed 29 March 2021.
3. Ministry of Finance of the People's Republic of China, Notice on improving the promotion and application of financial subsidy policies for new energy vehicles. http://jjs.mof.gov.cn/zhengcefagui/202004/t20200423_3502975.htm. Accessed 22 July 2020.
4. European Environment Agency, Fiscal instruments favouring electric over conventional cars are greener. <https://www.eea.europa.eu/publications/fiscal-instruments-favouring-electric-over>. Accessed 1 June 2020.
5. Center for Climate and Energy Solutions, U.S. state clean vehicle policies and incentives. <https://www.c2es.org/document/us-state-clean-vehicle-policies-and-incentives/>. Accessed 1 May 2020.
6. Transport Canada, Zero-emission vehicles. <https://www.tc.gc.ca/en/services/road/innovative-technologies/zero-emission-vehicles.html>. Accessed 1 June 2020.
7. International Energy Agency, World energy model. <https://www.iea.org/reports/world-energy-model/stated-policies-scenario>. Accessed 17 May 2020.
8. R. E. Ciez, J. F. Whitacre, Examining different recycling processes for lithium-ion batteries. *Nat. Sustain.* **2**, 148 (2019).
9. E. A. Olivetti, G. Ceder, G. G. Gaustad, X. Fu, Lithium-ion battery supply chain considerations: Analysis of potential bottlenecks in critical metals. *Joule* **1**, 229–243 (2017).
10. C. Helbig, A. M. Bradshaw, L. Wietschel, A. Thorenz, A. Tuma, Supply risks associated with lithium-ion battery materials. *J. Clean. Prod.* **172**, 274–286 (2018).
11. C. Vaalma, D. Buchholz, M. Weil, S. Passerini, A cost and resource analysis of sodium-ion batteries. *Nat. Rev. Mater.* **3**, 1–11 (2018).
12. B. Ballinger *et al.*, The vulnerability of electric vehicle deployment to critical mineral supply. *Appl. Energy* **255**, 113844 (2019).
13. G. Harper *et al.*, Recycling lithium-ion batteries from electric vehicles. *Nature* **575**, 75–86 (2019).
14. L. Gaines, Lithium-ion battery recycling processes: Research towards a sustainable course. *Sustainable Mater. Technol.* **17**, e00068 (2018).
15. X. Zhang *et al.*, Toward sustainable and systematic recycling of spent rechargeable batteries. *Chem. Soc. Rev.* **47**, 7239–7302 (2018).
16. H. Hao *et al.*, Impact of transport electrification on critical metal sustainability with a focus on the heavy-duty segment. *Nat. Commun.* **10**, 5398 (2019).
17. J. Schoch, J. Gaerttner, A. Schuller, T. Setzer, Enhancing electric vehicle sustainability through battery life optimal charging. *Transp. Res. Part B Methodol.* **112**, 1–18 (2018).
18. M. Shafie-Khah *et al.*, Optimal trading of plug-in electric vehicle aggregation agents in a market environment for sustainability. *Appl. Energy* **162**, 601–612 (2016).
19. Y. Xu, S. Çolak, E. C. Kara, S. J. Moura, M. C. González, Planning for electric vehicle needs by coupling charging profiles with urban mobility. *Nat. Energy* **3**, 484–493 (2018).
20. S. Wang, Z. Y. Dong, F. Luo, K. Meng, Y. Zhang, Stochastic collaborative planning of electric vehicle charging stations and power distribution system. *IEEE Trans. Industr. Inform.* **14**, 321–331 (2017).
21. H. Zhang, Z. Hu, Z. Xu, Y. Song, Optimal planning of PEV charging station with single output multiple cables charging spots. *IEEE Trans. Smart Grid* **8**, 2119–2128 (2016).
22. J. H. Teng, S. H. Liao, C. K. Wen, Design of a fully decentralized controlled electric vehicle charger for mitigating charging impact on power grids. *IEEE Trans. Ind. Appl.* **53**, 1497–1505 (2016).
23. M. Muratori, Impact of uncoordinated plug-in electric vehicle charging on residential power demand. *Nat. Energy* **3**, 193–201 (2018).
24. S. Habib, M. Kamran, U. Rashid, Impact analysis of vehicle-to-grid technology and charging strategies of electric vehicles on distribution networks—A review. *J. Power Sources* **277**, 205–214 (2015).
25. X. Chen *et al.*, Impacts of fleet types and charging modes for electric vehicles on emissions under different penetrations of wind power. *Nat. Energy* **3**, 413–421 (2018).
26. F. Knobloch *et al.*, Net emission reductions from electric cars and heat pumps in 59 world regions over time. *Nat. Sustain.* **3**, 437–447 (2020).
27. M. A. M. Tamayao, J. J. Michalek, C. Hendrickson, I. M. Azevedo, Regional variability and uncertainty of electric vehicle life cycle CO₂ emissions across the United States. *Environ. Sci. Technol.* **49**, 8844–8855 (2015).
28. Z. Wu *et al.*, Life cycle greenhouse gas emission reduction potential of battery electric vehicle. *J. Clean. Prod.* **190**, 462–470 (2018).
29. W. Ke *et al.*, Assessing the future vehicle fleet electrification: The impacts on regional and urban air quality. *Environ. Sci. Technol.* **51**, 1007–1016 (2017).
30. E. Ferrero, S. Alessandrini, A. Balanzino, Impact of the electric vehicles on the air pollution from a highway. *Appl. Energy* **169**, 450–459 (2016).
31. M. Tobollik *et al.*, Health impact assessment of transport policies in Rotterdam: Decrease of total traffic and increase of electric car use. *Environ. Res.* **146**, 350–358 (2016).
32. X. Liang *et al.*, Air quality and health benefits from fleet electrification in China. *Nat. Sustain.* **2**, 962–971 (2019).
33. R. Basso, B. Kulcsár, B. Egardt, P. Lindroth, I. Sanchez-Diaz, Energy consumption estimation integrated into the electric vehicle routing problem. *Transp. Res. Part D Transp. Environ.* **69**, 141–167 (2019).
34. X. Yuan, L. Li, H. Gou, T. Dong, Energy and environmental impact of battery electric vehicle range in China. *Appl. Energy* **157**, 75–84 (2015).
35. L. C. Casals, E. Martinez-Laserna, B. A. Garcia, N. Nieto, Sustainability analysis of the electric vehicle use in Europe for CO₂ emissions reduction. *J. Clean. Prod.* **127**, 425–437 (2016).
36. X. Yuan, C. Zhang, G. Hong, X. Huang, L. Li, Method for evaluating the real-world driving energy consumptions of electric vehicles. *Energy* **141**, 1955–1968 (2017).
37. D. Hall, H. Cui, N. Lutsey, *Electric Vehicle Capitals: Accelerating the Global Transition to Electric Drive* (The International Council on Clean Transport, Washington, DC, 2018).
38. T. Franke, M. Günther, M. Trantow, J. F. Krems, Does this range suit me? Range satisfaction of battery electric vehicle users. *Appl. Ergon.* **65**, 191–199 (2017).
39. Z. Li *et al.*, Battery capacity design for electric vehicles considering the diversity of daily vehicles miles traveled. *Transp. Res. Part C Emerg. Technol.* **72**, 272–282 (2016).
40. A. I. Stroe, V. Knap, D. I. Stroe, Comparison of lithium-ion battery performance at beginning-of-life and end-of-life. *Microelectron. Reliab.* **88**, 1251–1255 (2018).
41. S. Ma *et al.*, Temperature effect and thermal impact in lithium-ion batteries: A review. *Prog. Nat. Sci.* **28**, 653–666 (2018).
42. M. Jafari, A. Gauchia, S. Zhao, K. Zhang, L. Gauchia, Electric vehicle battery cycle aging evaluation in real-world daily driving and vehicle-to-grid services. *IEEE Trans. Transp. Electrification* **4**, 122–134 (2017).
43. S. Ou *et al.*, Light-duty plug-in electric vehicles in China: An overview on the market and its comparisons to the United States. *Renew. Sustain. Energy Rev.* **112**, 747–761 (2019).
44. K. Hyatt, S. Ewing, Here's every electric vehicle on sale in the US for 2020 and its range. <https://www.cnet.com/roadshow/news/every-electric-car-ev-range-audi-chevy-tesla/>. Accessed 5 July 2020.
45. P. Plötz, N. Jakobsson, F. Sprei, On the distribution of individual daily driving distances. *Transp. Res., Part B: Methodol.* **101**, 213–227 (2017).
46. N. S. Pearce, W. Kempton, R. L. Guensler, V. V. Elango, Electric vehicles: How much range is required for a day's driving? *Transp. Res., Part C Emerg. Technol.* **19**, 1171–1184 (2011).
47. D. Rufiange, Tesla working on 400 miles (643 km) of range from improved batteries. <https://www.cnet.com/roadshow/news/every-electric-car-ev-range-audi-chevy-tesla/>. Accessed 1 May 2020.
48. Z. A. Needell, J. Mc Nerney, M. T. Chang, J. E. Trancik, Potential for widespread electrification of personal vehicle travel in the United States. *Nat. Energy* **1**, 16112 (2016).
49. Y. Gao *et al.*, Lithium-ion battery aging mechanisms and life model under different charging stresses. *J. Power Sources* **356**, 103–114 (2017).
50. C. Y. Wang *et al.*, Lithium-ion battery structure that self-heats at low temperatures. *Nature* **529**, 515–518 (2016).
51. J. Lindgren, P. D. Lund, Effect of extreme temperatures on battery charging and performance of electric vehicles. *J. Power Sources* **328**, 37–45 (2016).
52. X. Shen, H. Liu, X. B. Cheng, C. Yan, J. Q. Huang, Beyond lithium ion batteries: Higher energy density battery systems based on lithium metal anodes. *Energy Storage Mater.* **12**, 161–175 (2018).
53. T. Yuksel, J. J. Michalek, Effects of regional temperature on electric vehicle efficiency, range, and emissions in the United States. *Environ. Sci. Technol.* **49**, 3974–3980 (2015).
54. K. Liu, J. Wang, T. Yamamoto, T. Morikawa, Exploring the interactive effects of ambient temperature and vehicle auxiliary loads on electric vehicle energy consumption. *Appl. Energy* **227**, 324–331 (2018).
55. Idaho National Laboratory, Advanced vehicles: Data. <https://avt.inl.gov/project-type/data>. Accessed 1 February 2019.
56. Argonne National Laboratory, Data from "Electric vehicle testing." Downloadable Dynamometer Database. <https://www.anl.gov/es/electric-vehicle-testing>. Accessed 1 January 2019.
57. J. Taggart, "Ambient temperature impacts on real-world electric vehicle efficiency & range" in *2017 IEEE Transportation Electrification Conference and Expo (ITEE, 2017)*, pp. 186–190.
58. National Bureau of Statistics, Electricity generation by province and month. <http://data.stats.gov.cn/easyquery.htm?cn=E0101>. Accessed 1 February 2020.
59. C. Fiori, K. Ahn, H. A. Rakha, Power-based electric vehicle energy consumption model: Model development and validation. *Appl. Energy* **168**, 257–268 (2016).
60. J. Schäuble, T. Kaschub, A. Ensslen, P. Jochem, W. Fichtner, Generating electric vehicle load profiles from empirical data of three EV fleets in southwest Germany. *J. Clean. Prod.* **150**, 253–266 (2017).